

СООБЩЕНИЯ  
ОБЪЕДИНЕННОГО  
ИНСТИТУТА  
ЯДЕРНЫХ  
ИССЛЕДОВАНИЙ

Дубна

97-106

E3-97-106

INVESTIGATIONS OF THE PARITY VIOLATION  
AND INTERFERENCE EFFECTS IN  $^{235}\text{U}$  FISSION  
INDUCED BY RESONANCE NEUTRONS

1997

V.P.Alfimenkov, A.N.Chernikov, L.Lason\*, Yu.D.Mareev, V.V.Novitski,  
L.B.Pikelner, V.R.Skoy, M.I.Tsulaya  
*Frank Laboratory of Neutron Physics, JINR, Dubna, Russia*

A.M.Gagarski, I.S.Guseva, S.P.Golosovskaya, I.A.Krasnoschokova,  
A.M.Morozov, G.A.Petrov, V.I.Petrova, A.K.Petukhov, Yu.S.Pleva,  
V.E.Sokolov, G.V.Val'ski  
*Neutron Research Department, PNPI of RAS, Gatchina, Russia*

S.M.Soloviev  
*Khlopin Radium Institute, Sankt-Petersburg, Russia*

Space parity nonconservation (PNC) in thermal neutron induced fission of  $^{233,235}\text{U}$  and  $^{239}\text{Pu}$  has been observed in 1976/1977 [1] in the investigations of light (heavy) fragment angular distributions relative to the neutron spin direction. In more recent time, the PNC-effects were also measured in the cold neutron induced fission of  $^{229}\text{Th}$ ,  $^{241}\text{Pu}$  and  $^{241}\text{Am}$  [2].

In all of these cases, the PNC-effects have been found to be surprisingly large  $(1 - 7) \cdot 10^{-4}$  in spite of averaging over huge numbers of fission fragment final states. In subbarrier fission of  $^{237}\text{Np}$  and  $^{245}\text{Cm}$  fission, the PNC-effect values are probably less than  $1 \cdot 10^{-4}$  [3].

The first theory of PNC-effects in nuclear fission were proposed by Sushkov and Flambaum [4] and Bunakov and Gudkov [5]. The authors of these works used the assumption about mixing neighbouring compound-states with opposite parities by the weak nucleon-nucleon interaction. As is well known, the same supposition was used before [6] to explain the PNC-effect arising in  $(n,\gamma)$ -reactions.

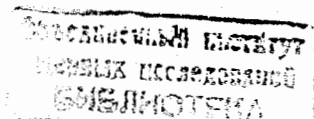
As a result of such a mixing, the interference between the final fission channels with even and odd orbital momenta can appear. In turn, this interference leads to the asymmetry of the light (heavy) fragment emission relative to the spin direction of polarized neutrons - initiated nuclear fission. Because of the binary type of the reaction, the asymmetry coefficients for the light and heavy fragments have opposite signs.

It seemed that because the PNC-effect magnitudes and signs should fluctuate randomly for different exit channels, the averaged PNC-effect value observed in the experiments should have been very small. But, as mentioned above, this is not the case, because in fission, the role of real exit channels play not numerous fragment final states, but a few A.Bohr transition states near the top of the fission barrier (see, e.g., [7]). As a result, no strong dependence of the PNC-effect on individual fragment characteristics is was expected in the framework of the theory [4,5,7].

Moreover, it was assumed [4,5] that the well known (in the nuclear physics) parity conserving (PC) interference effects of left-right (LR) and forward-backward (FB) asymmetry of the reaction product (in our case, fragment) emission have many similarities with the PNC effect in the way these effects arise in the fission process. As a result, joint investigations of the PNC and PC interference effects can essentially extend the capabilities of the theoretical analysis of experimental data. However, the practical implementation of such a possibility has met with serious difficulties. First of all, because of very high level density in the excited fissile nuclei ( $\bar{\Gamma} \sim \bar{D}$ ), usually several compound-states with different spins and parities may be involved in the way interference effects arise. So far, accurate analysis of effects need detailed information on many excited levels. But to perform such experiment, high fluxes of resonance polarized neutrons ( $\Phi_n > 10^4 \text{ n/cm}^2 \cdot \text{s} \cdot \text{eV}$ ) are necessary, and the quantity of the fissile isotope has to be not less than some grams. These very strong requirements were the main reason PNC-effects were measured only for thermal neutrons [1,2,3] or in a very narrow neutron energy range ( $E_n \leq 0.6$ ) eV [8,9,10].

Nevertheless, these first investigations have confirmed some important theoretical suppo-

\*Permanent address: Department of Nuclear Physics, Lodz University, Poland



sitions. In particular they gave additional arguments in favour of the decisive role of the compound-stage of the fissioning system for the appearance of the PNC-effect and demonstrated a fruitfulness of a joint study of the PNC and PC interference effects, as well as the possibility of getting new information about compound-state characteristics as a result.

The main aim of this work is to extend the neutron energy range of the PNC and PC interference effect investigations as compared with the previous work [8,9,10] and in joint theoretical analysis of all results obtained. These investigations have become possible because of the high polarized neutron flux at the IBR-30 reactor and the new design of the multisectioned ionization chambers with 2 grams of  $^{235}\text{U}$  fissile isotope.

Isotope  $^{235}\text{U}$  was chosen for these investigations, taking into account the fact that neutron resonance parameters are relatively well known for this isotope from numerous experiments, including investigations with polarized neutrons and nuclei [11]. In addition, the natural  $\alpha$ -activity of  $^{235}\text{U}$  is relatively low as compared with the other fissile isotopes, which is very important in measuring fission fragment energies in the presence of high  $\alpha$ -particle intensities. This allowed the use of such a great amount of fissile material.

## 1 Some essential features of the theory of PNC and PC interference effects in fission fragment angular distributions

The angular distributions of the light (or heavy) fission fragments are described by the expression:

$$W(\theta, \varphi) = 1 + \alpha_{nf} \cdot (\vec{\sigma}_n \cdot \vec{p}_f) + \alpha_{nf}^{lr} \cdot (\vec{\sigma}_n \cdot [\vec{p}_n \times \vec{p}_f]) + \alpha_{nf}^{fb} \cdot (\vec{p}_n \cdot \vec{p}_f) \quad (1)$$

where  $\vec{p}_f$  and  $\vec{p}_n$  are the unit vectors of linear momenta for the light fragments and neutrons,  $\vec{\sigma}_n$  is the unit pseudovector of neutron polarization, and  $\alpha_{nf}$ ,  $\alpha_{nf}^{lr}$  and  $\alpha_{nf}^{fb}$  are the PNC and PC LR and FB asymmetry coefficients for the light fission fragment group.

The aim of our measurements was to determine the  $\alpha$  coefficients, which are the functions of neutron energy, and the parameters of s- and p-wave resonances. Simultaneous fitting of all experimental data can give information about the parameters of the p-resonances of  $^{235}\text{U}$  and matrix elements of the weak interaction. Up to now, such information is entirely absent.

The principal characteristic feature of angular distributions as (1) is that all of them contain the first power spherical harmonics. It is common knowledge from the nuclear reaction theory that the presence in reaction products angular distributions the odd power spherical harmonics, strongly suggests that the reaction examined goes through more than one intermediate state with definite parity. For the PC interference effects, the compound-states with opposite parities may be excited in the process of s- and p-wave neutron capture ( $l = 0; 1$ ). The spins and parities of such states are determined as follows:

$$\vec{J} = \vec{I} + \vec{s} + \vec{l} = \vec{I} + \vec{j}, \quad \pi_J = (-1)^l \cdot \pi_I$$

where  $\vec{J}$  and  $\vec{I}$  are the spins of compound and target nuclei respectively,  $\vec{s}$  and  $\vec{l}$  are the spin and orbital momentum of neutron, and  $\pi_J$  and  $\pi_I$  are the parities of the compound and target nuclei, respectively.

In principle, the PNC-effect can arise, and with s-wave neutron capture. In this case, some close p-wave states may be admixed to the s-state by the weak interaction. In all cases mentioned above, the intermediate state in the neutron reaction will have indefinite parity and the two fission fragments with fixed parameters will have both odd and even orbital momenta as a result. Corresponding correlation functions turn out to be very complicated even in the case of only two mixing compound-states. In particular, the interference terms are functions of the complex matrix element phases and depend very strongly on the neutron energies. In the limit of a large number of mixed compound-states, a mutual compensation of such interference terms may come as a result. In this case, the correlation function will be close to zero or may have only even powers of the spherical harmonics. A similar suppression of interference effects was a result of averaging the effects over huge numbers of fragment final states. But, as it was explained in introduction, this was not observed because of some peculiarity of the low energy fission reaction.

Taking into account all of these physical notions, the following general equations for the PNC and PC asymmetry coefficients can be written on the basis of the theoretical works of Sushkov and Flambaum [4] and Bunakov and Gudkov [5]:

$$\alpha_{nf}^{fb}(E) = \frac{1}{\Delta E \cdot \sigma(E)} \int_{E-\Delta E/2}^{E+\Delta E/2} \left[ \sum_{spj} Q(J_s J_p j K I) \cdot \Re(U_s U_{pj}^*) \right] dE' \quad (2)$$

$$\alpha_{nf}^{lr}(E) = \frac{1}{\Delta E \cdot \sigma(E)} \int_{E-\Delta E/2}^{E+\Delta E/2} \left[ \sum_{spj} Q(J_s J_p j K I) \cdot \Im(\beta U_s U_{pj}^*) \right] dE' \quad (3)$$

$$\alpha_{nf}(E) = \frac{1}{\Delta E \cdot \sigma(E)} \int_{E-\Delta E/2}^{E+\Delta E/2} \left[ \sum_{ss'p} Q(J_p J_s, \frac{1}{2} K I) \cdot \Re(U_{sp} U_{s'}^*) \right] dE' \quad (4)$$

where  $j$  is total neutron angular momentum and  $J_s, J_{s'}, J_p$  are the s- and p-resonance spins,

$$U_s = \frac{A_s(J_s) \cdot F_s}{E' - E_s + i\Gamma_s/2}, \quad U_{pj} = \frac{A_p(J_p, j) \cdot F_p}{E' - E_p + i\Gamma_p/2}, \quad (5)$$

$A_s(J_s) = \sqrt{\Gamma(J_s)} e^{i\psi_s^l}$ , and  $A_p(J_p, j) = \sqrt{\Gamma(J_p, j)} e^{i\psi_p^j}$  are the neutron capture amplitudes for s- and p-resonances,  $F_s, F_p$  are the fission amplitudes for s- and p-resonances, and

$$\beta = \begin{cases} 1 & \text{if } j = 1/2, \\ -1/2 & \text{if } j = 3/2, \end{cases}$$

$$U_{sp} = \frac{A_s(J_s) \langle p | I | s \rangle F_p}{(E' - E_s + i\Gamma_s/2) \cdot (E' - E_p + i\Gamma_p/2)}, \quad (6)$$

where  $\Delta E$  is the energy average interval,  $\sigma(E)$  is the fission cross section, and

$$Q(J_s J_p j K I) = 2\sqrt{3}(2J_s + 1)(2J_p + 1)\sqrt{2j + 1} \cdot (-1)^{1+j-l-K} \times \\ \times \begin{Bmatrix} \frac{1}{2} & 1 & j \\ J_p & I & J_s \end{Bmatrix} \begin{pmatrix} J_s & J_p & 1 \\ K & -K & 0 \end{pmatrix} \quad (7)$$

It is evident that these equations have definite similarities in the dependences of the PNC and PC asymmetry coefficients on the s- and p-resonance parameters.

## 2 Experimental installation and measurement procedures

### 2.1 Pulsed neutron source

All measurements of the PNC and PC asymmetry coefficients as functions of the resonance neutron energies in  $^{235}\text{U}$  fission were carried out on the beams of the IBR-30 pulsed reactor, operated as a booster with the LUE-40 electron linear accelerator [12]. Initial neutrons are produced by electron interaction with a tungsten target placed in the active core of the IBR-30 reactor. The standard frequency of the two-sectioned LUE-40 accelerator is 100 Hz, with an electron energy of 40 MeV and an electron pulse current of about 0.4 A. A high coefficient of neutron multiplication (up to 200) is achieved when the flush of fast neutrons from the tungsten target coincides with the maximum of IBR-30 reactivity. Fast neutrons are moderated in a water moderator and then fly through a vacuum tube to the experimental installations.

The average power of the booster is equal to 10 kW and the effective width of a neutron pulse is about 4  $\mu\text{s}$ .

Measurements were fulfilled by the time-of-flight method.

### 2.2 Forward-backward asymmetry measurement

The PC FB asymmetry measurement was carried out on the neutron beam No. 1 of the IBR-30 at a flight path of 33 m. For fission fragment registration, a multisectioned fast ionization chamber was constructed. This type of fission detector was chosen for our experiments, taking into account the following requirements:

1. The detector system has to provide a partitioning of the fragment kinetic energy spectra into two groups peculiar to the light and heavy mass groups.
2. To achieve the needed statistical accuracy of the experimental results in an acceptable time, the total amount of fissile isotopes investigated has to be not less than some grams.
3. Because of the very high specific ionization of the charged fission fragments and high background of the target  $\alpha$ -activity, the thickness of the fissile material layers must be not much less than 0.4 mg/cm<sup>2</sup>.
4. The dead time of the detector and electronics cannot be worse than a fraction of a microsecond. A schematic view of this chamber is shown in Fig 1.; its detailed description can be found in [14].

The detector consists of 16 sections, each is included in two elementary chambers with a common cathode having two anodes 10 mm distant from it. Each section was shielded from the two neighbouring ones by grounded plates. All electrodes were made of aluminium foils of 0.3 mm in thickness and 310 mm in diameter. The double-sided layers of  $^{235}\text{U}$  oxide were coated on the cathodes with an active spot diameter of 230 mm and thickness of about 0.15 mg/cm<sup>2</sup>. The total amount of fissile material was about 2 g. The whole volume of the detector was filled with isobutane at 0.7 atm.

In the course of measurements, the geometrical axis of the multisectioned ionization chamber had two possible orientations along the neutron beam, which was changed every 200 seconds by a computer-controlled mechanical driver.

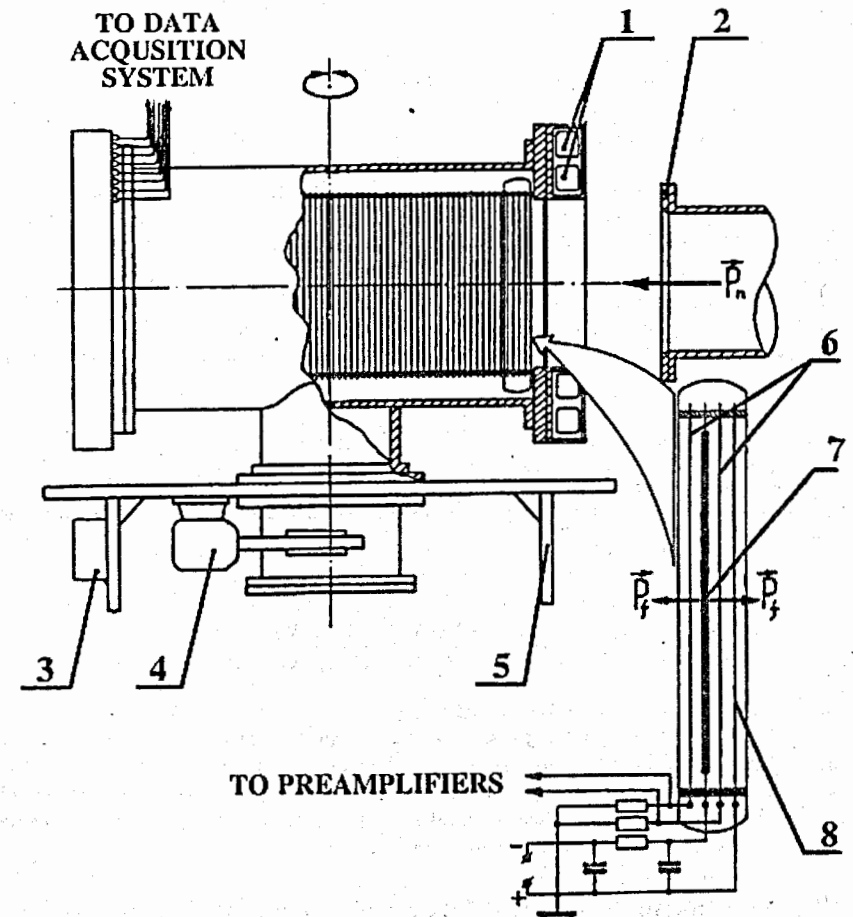


Figure 1: Schematic view of multisectioned ionization chamber used for the forward-backward asymmetry measurements: 1 - preamplifiers, 2 - neutron guide, 3 - automatic control unit, 4 - driving motor, 5 - chamber support. Below from the right - schema of ionization chamber section: 6 - anodes of the section, 7 - joint cathode-target, 8 - screen plate (see text).



The solid angle of the fragment registration was close to  $2\pi$ , with average directions of fragment emission being mutually opposite for two elementary chambers in each section.

For measurement of the fragment energy and time-of-flight spectrum, a hardware system was created in CAMAC standard. It included 32 similar spectrometric lines to measure the fragment kinetic energy spectra, a time converter, two buffer memories, and IN and OUT registers.

The multiparameter events accumulated in experiments had the following characteristics:

- markers of the light and heavy fragment group (2),
- markers of chamber position (2),
- numbers of elementary ionization chambers (or groups, if connected) (32),
- channel numbers of the neutron time-of-flight spectra (1024).

Such multiparameter events were collected by the hardware environment in the buffer memory over a time of about 7 milliseconds between two neighbouring start reactor pulses. Then the content of the buffer memory was forwarded to an IBM PC AT-386 by the DMA channel for further data sorting and restoring. To minimize the event count losses, a double buffering was used in the system, such that the events accumulation from each successive reactor start was sent to the second memory before the first one was read out.

As seen from Eq. (1), the coefficient of FB asymmetry can be obtained from the experimental data using formula:

$$\alpha_{\text{exp}} = \frac{N_L^1 - N_L^2}{N_L^1 + N_L^2} \quad (8)$$

where  $N_L^1$  are the light fragment count rates for two opposite directions of escape. However, turning the chamber slightly changed the experimental conditions, so another formula was used:

$$\alpha_{\text{exp}} = \frac{(N_L/N_H)^1 - (N_L/N_H)^2}{(N_L/N_H)^1 + (N_L/N_H)^2} \quad (9)$$

where  $N_H$  is the count rate of heavy fragments.

In Fig 2, one of the time-of-flight spectra obtained in the forward-backward measurement is shown. Experimental results were corrected for the length of the chamber (60 cm), background, overlapping of light and heavy groups of fission fragments in the amplitude spectrum (10%), and for the solid angle of fragment registration. Thereafter, the energy dependence of the  $\alpha_{nf}^b$  coefficient was obtained. This is shown in Fig 3(A).

### 2.3 Measurements of the left-right asymmetry and PNC effects in $^{235}\text{U}$ fission

Measurements of the left-right asymmetry and parity violation effects require a beam of polarized resonance neutrons. This is available on the beam No. 4 of IBR-30 where facility POLYANA [13] is placed.

Resonance polarized neutrons were obtained by the method of neutron transmission through the polarized proton target, consisted of monocrystal  $\text{La}_2\text{Mg}_3(\text{NO}_3)_{12}\cdot 24\text{H}_2\text{O}$  with the area about  $30 \text{ cm}^2$  and thickness about 17 mm. The protons in crystallized water were polarized by the solid-effect method. The monocrystal was placed in a 2 T magnetic field and in super-high-frequency field with the wave length 4.2 mm a temperature of about 1° K.

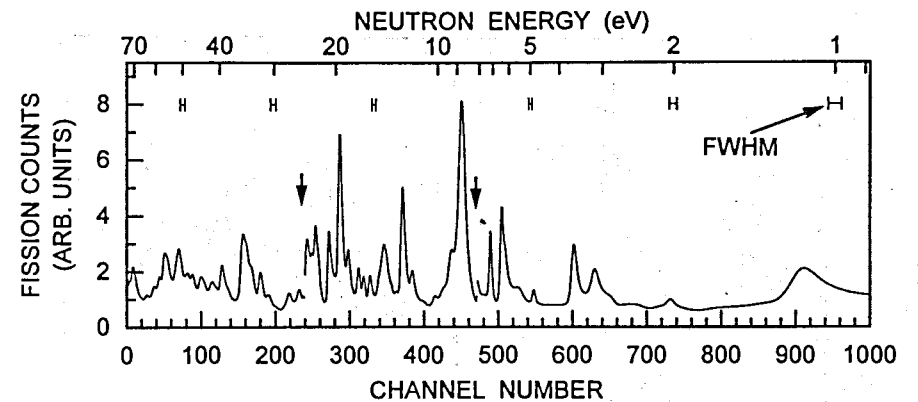


Figure 2: One of time-of-flight spectra obtained in the investigations of the PC forward-backward asymmetry.

The polarized proton target is part of the facility "POLYANA", which is shown in Fig 4. The target was situated at a distance of 9 m from the neutron moderator surface. The flux of resonance polarized neutrons passing from the proton target at the rated power of IBR-30 was about  $3 \cdot 10^5 \cdot E^{-0.9} \text{ n/s-eV}$ .

Fast reverse of the neutron polarization was executed when reversing the current in one of the magnets of guiding magnetic fields. At the standard mode of proton target operation the average polarization over whole neutron energy region investigated was about 60%.

In LR and PNC effect measurements, the fission fragments must be detected when they move perpendicular to the neutron momenta. Therefore, a special chamber was designed and its schematic view is shown in Fig 5.

The general principles of this chamber design and operation were the same as for the first one above. Its constructional peculiarities were motivated by the geometry of the polarized neutron beam (the spot of  $70 \times 70 \text{ mm}^2$ ) and the pole gap of the electromagnet where the multisectioned ionization chamber had to be placed. As a result, unlike the first chamber, the second had 40 sections with right-angle formed electrodes ( $110 \times 96 \text{ mm}^2$ ) made of 0.15 mm-thickness aluminium foil. Fissile layers had an average thickness about  $0.35 \text{ mg/cm}^2$ , such that the total amount of  $^{235}\text{U}$  isotope was the same as in the first chamber (about 2 g). These were lined up with neutron beam direction. Whole volume of this chamber was filled with an Ar + 5%CH<sub>4</sub> gas mixture at 2.4 atm instead of isobutane at 0.7 atm in the first chamber. This change of the counting gas was done to decrease the background of the scattered neutrons. The flight path for this chamber was about 13 m.

Measurements of the LR and PNC effects have some advantages over the FB measurement as chamber did not turn and only the neutron polarization changed sign. Thus formula (8) can be used for analysis of the experimental results. Except for the polarization, which was reversed every 100 sec., the other procedures were the same as in the FB measurements. The left-right and PNC asymmetry coefficients  $\alpha_{nf}^l$  and  $\alpha_{nf}$  are shown in Fig 3(B,C) and Fig 6(B,C).

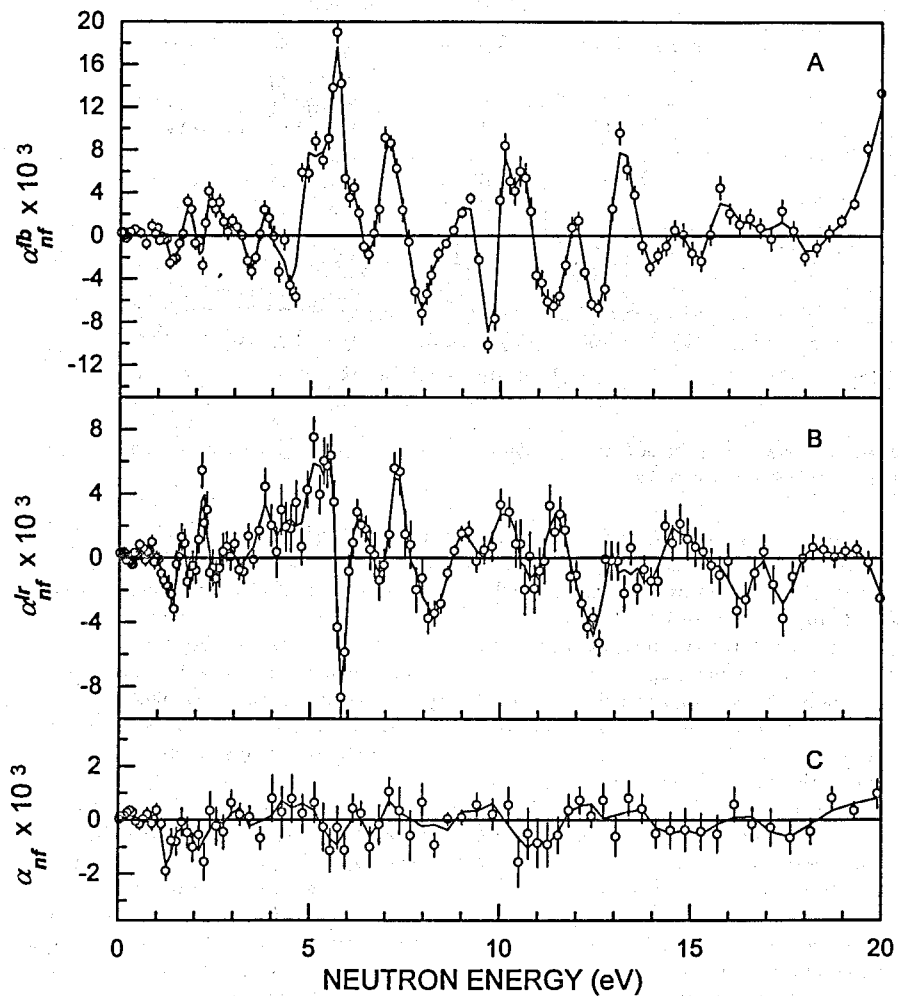


Figure 3: Parity conserving forward-backward (A), left-right (B) and parity violating (C) interference effects of asymmetry of fission fragment emission as function of neutron energies for the range (0.02 — 20) eV. The curves are to guide the eye.

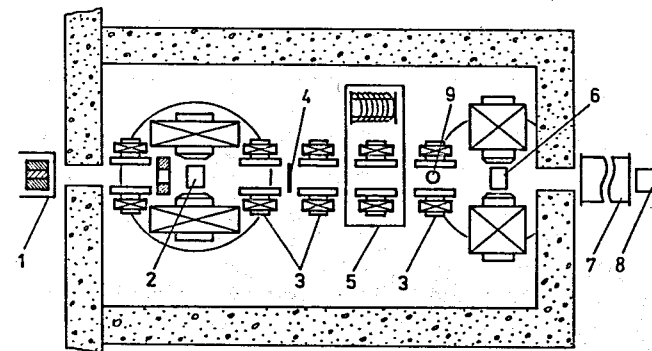


Figure 4: Schema of the installation for polarized neutron producing "POLYANA" at the IBR-30 fast pulsed reactor. 1 - reactor core, 2 - polarized proton target with  $\text{La}_2\text{Mg}_3(\text{NO}_3)_{12} \cdot 24\text{H}_2\text{O}$  monocrystal, 3 - magnets of a guiding field, 4 - foil with direct current, 5 - interchangeable magnet, 6 - multisectioned ionization chamber, 7 - vacuum tube, 8 - neutron monitor.

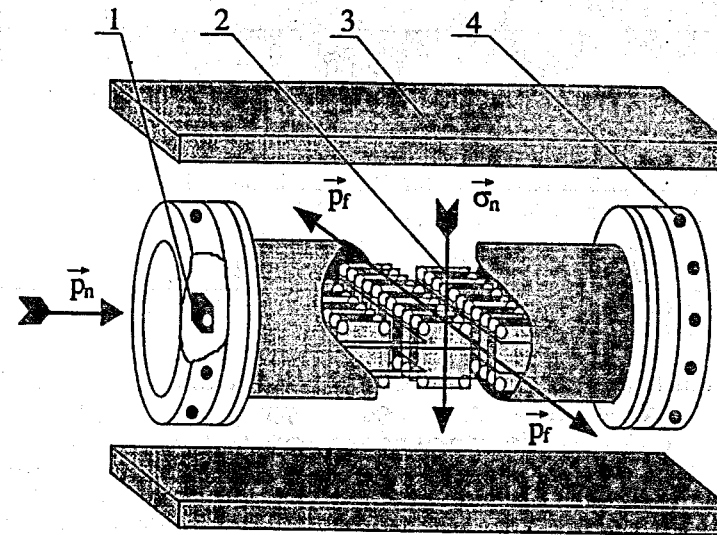


Figure 5: Schematic view of the second multisectioned ionization chamber used for the PNC and PC left-right asymmetry measurements: 1 - preamplifiers, 2 - the row of five chamber sections, 3 - magnet poles of a guiding field, 4 - outputs of preamplifiers (see text).

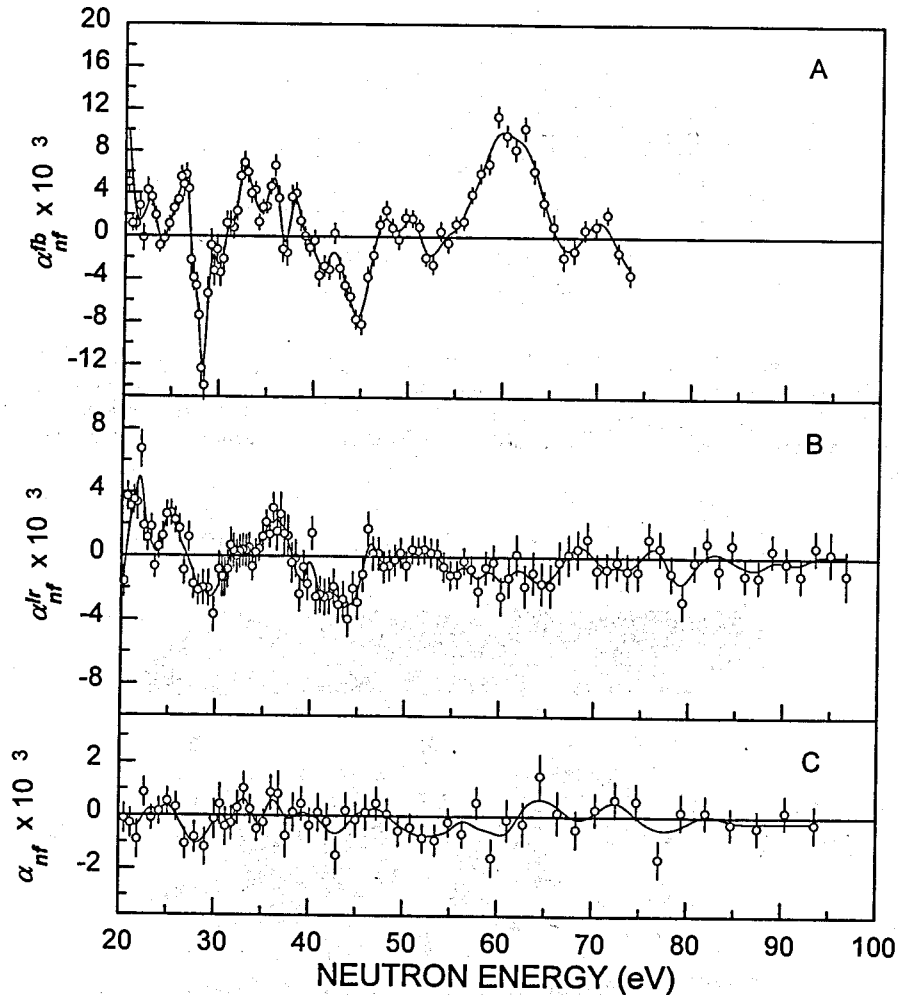


Figure 6: Parity conserving forward-backward (A), left-right (B) and parity violating (C) interference effects of asymmetry of fission fragment emission as a function of neutron energies for the range (20 — 100) eV. The curves are to guide the eye.

### 3 The main experimental results

As pointed out above, the experimental investigations of PNC and PC (LR) asymmetry of fission fragment emission were performed for neutrons with energies within the range (0.02 — 90) eV and measurements of the PC (FB) asymmetry coefficients as a function of neutron energy within the range (0.02 — 70) eV.

Neutron energy dependences of the PC FB and LR and the PNC asymmetry coefficients are shown in the Figs. 3, 6 and 7 (parts A, B, and C, respectively). The curves shown in the figures were drawn for better visualization of the data obtained.

It is interesting to point out some general characteristics of the asymmetry coefficients as functions of neutron energies presented in the Figs. 3 and 6.

First, the neutron energy dependences of the PC FB and LR asymmetry coefficients were found to have well-marked irregularities over whole energy range investigated. Values of the FB and LR coefficients, averaged with the weights over energy intervals of equal 10 eV widths are shown in Table 1.

$\Delta E(\text{eV})$	$\bar{\alpha}_{nf}^{fb} \cdot 10^4$	$\bar{\alpha}_{nf}^{lr} \cdot 10^4$	$\bar{\alpha}_{nf} \cdot 10^4$
0÷10	3.14±0.44	1.83±0.25	0.83±0.22
10÷20	1.8±1.3	-5.8±1.3	0.6±1.2
20÷30	7.8±1.8	10.8±1.9	-0.8±1.6
30÷40	25.6±1.8	3.9±1.9	0.7±1.7
40÷50	-21.5±2.2	-11.9±2.4	-1.7±2.1
50÷60	21.2±2.3	-3.9±2.4	-5.5±2.1
60÷70	22.2±2.8	-6.8±3.7	2.4±3.2
70÷80	-	-6.1±3.6	-1.1±3.2
80÷95	-	-2.1±3.1	-1.0±2.9
0÷95	-	1.47±0.24	0.70±0.21
0÷70	4.34±0.38	-	-
$\bar{\alpha}_{ar.m.}$	8.60	-2.23	-0.60

Table 1: Average weighted values of the asymmetry coefficients for the separated energy intervals of the equal width.

Secondly, the widths of observed peculiarities in the neutron energy dependence of the FB and LR asymmetry coefficients exceed, in many cases, the average widths of the s- and p-resonances, which overlapping brings into existence. [4,5]. The number of such peculiarities was found to be well below the average s- and p-resonance density expected from the known data [11]. Such features can arise as a result of the accidental overlapping of some neighbouring resonances such that the signs of the interference effects turn out to be the same. This conclusion was qualitatively confirmed in a direct computer simulation of the interference effects with s-resonance parameters being taken from well-known data [11], but the p-resonances were drawn randomly [16]. However, it is impossible to exclude completely the possibility of the existence some non-incidental sign correlation when interference effects arise in the fission reaction.

Thirdly, the statistical accuracy of the PNC effect measurements achieved in our investigations is not high enough to examine the behaviour of the  $\alpha_{nf}$  coefficient as a function of neutron energies for whole available interval. The resonance dependence of the PNC asymmetry coefficients was reliably observed in the vicinity of neutron energies 0.3 eV and 1.2 eV. The

effects have opposite signs and different magnitudes in the maxima. The PNC effect at 0.3 eV was observed for the first time in [10]. In the same article, the PC LR asymmetry effect was measured inside relatively narrow neutron energy range  $E_n < 0.6$  eV.

#### 4 Theoretical analysis of the data and discussion of results

The first demonstration of the possibility of getting a new important information about p-wave resonance properties in heavy fissile nuclei was obtained in the investigations of the FB asymmetry of fragment emission in  $^{233,235}\text{U}$  fission [18,19,20]. The preliminary estimates for the p-resonance parameters were presented in these publications.

The special attention in this paper is focused on the first joint theoretical analysis of the PC and PNC interference effects. For this analysis, we used the theoretical equations (2, 3, 4) obtained from the basis of the works of Suchkov and Flambaum [4] and Bunakov and Gudkov [5]. It can be seen from these equations that for a correct theoretical analysis, one needs all of the parameters of the mixing s- and p-resonances, namely:  $E_{s,p}$ ,  $\Gamma_{s,p}$ ,  $\Gamma_{s,p}^n$ ,  $\Gamma_{s,p}^f$ ,  $\Gamma_{p1/2}^n/\Gamma_{p3/2}^n$ ,  $J_{s,p}$ ,  $\Gamma_{s,p}^f(K)/\Gamma_{s,p}^f$ , and the phase factors  $\Delta\varphi_{sp}^f = \varphi_s^f - \varphi_p^f$ . In spite of the fact that  $^{235}\text{U}$  is the most investigated fissile isotope, the main resonance parameters needed are known only for the s-resonances [11], but even in this case, the information about such important parameters as partial fission widths for the transition states with different  $K$ -values are practically unknown. There is no definite information about the phase factors,  $\Delta\varphi_{sp}^f$  or about all parameters of low energy p-wave resonances as well. It is particularly necessary to point out here that in the works of Bunakov and Gudkov [5] and Barabanov and Furman [21], the value  $\Delta\varphi_{sp}^f = \pi/2$  was proposed for all cases of low energy-fission. In the contrast to these works, Sushkov and Flambaum [4] used  $\Delta\varphi_{sp}^f$  as the fitting parameters.

All of this, together with the very high compound-level density and relatively low statistical accuracy for the PNC effect, essentially complicates the combined theoretical analysis of the PNC and PC interference effects in fissile nuclei. Such an analysis is presently possible only for a narrow neutron energy region, where the PNC effect has very clearly defined peculiarities in the energy dependences.

For this reason, we have performed an analysis of experimental data obtained within two narrow ranges of neutron energies as follows: (0.02 — 1.6) eV and (5.2 — 6.6) eV. Inside the second neutron energy interval, the PNC effect was not clearly observed in our experiments, but the FB and LR asymmetry effects had very clear expressed peculiarities. About 20 s-resonances from the energy range (0.02 — 6.6) eV and the nearest neighborhood were taken into consideration in this analysis [11].

To make the theory fit the experimental data, two simplified assumptions were made as follows:

1. It was assumed that in most cases, the fission of all s- and p-resonances studied goes through the same transition states with  $K = 1$ . However, for the s-resonances with the energies of 0.29 eV and 2.028 eV  $K = 0$ , the preliminary Dubna results [22] were taken into account.

2. In view of the fact that only the phase difference  $\Delta\varphi_{sp}^f = \varphi_s^f - \varphi_p^f$  appears in the equations (2, 3, and 4), but not  $\varphi_s^f$  and  $\varphi_p^f$  separately, it was suggested that  $\varphi_s^f$  is the same for all s-resonances involved in the analysis. As a result we had only  $(n_p + 1)$  phase parameters, with  $n_p$  being the number of p-resonances in the neutron range investigated.

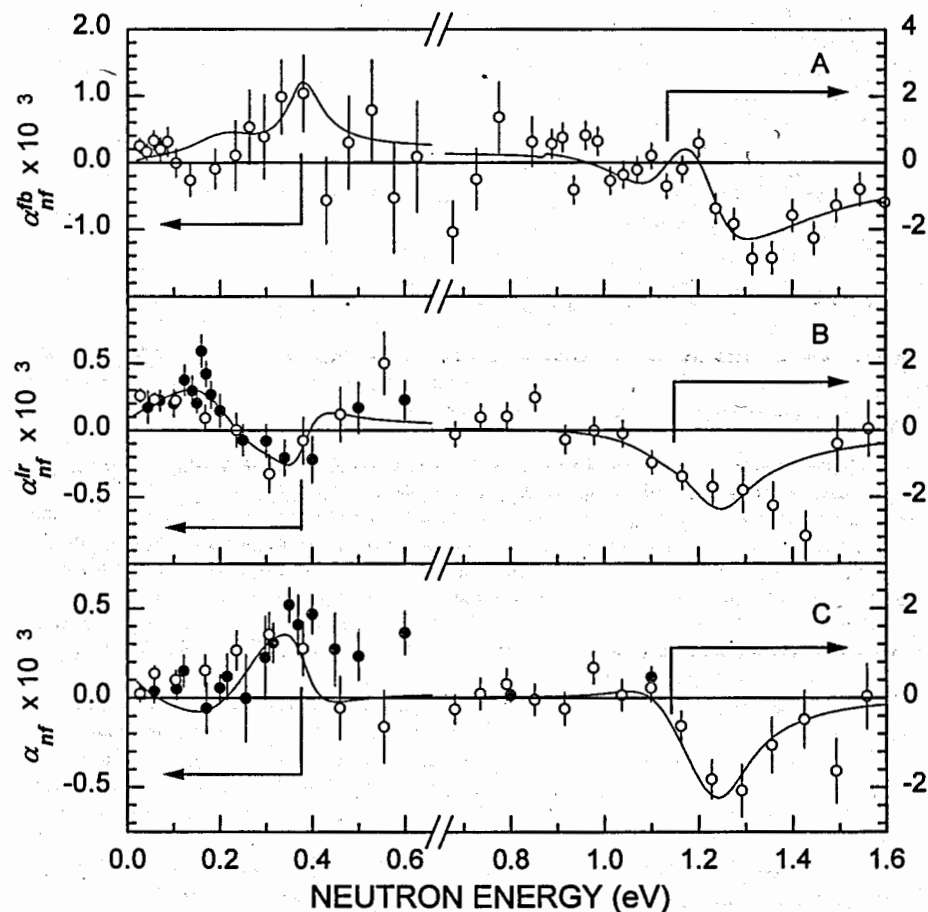


Figure 7: PC forward-backward (A), PC left-right (B) and PNC (C) interference effects of fission fragment emission as a function of neutron energy for the range (0.02 — 1.6) eV. The curve are the result of the theoretical fits.



The procedure of the theoretical fit was performed in two steps. At the first step, the theoretical equations (2, 3) were fitted to the experimental data for neutron energy dependence of the PC interference effects of FB and LR asymmetry of fission fragment emission. As a result, the main parameters of the p-wave resonances were extracted. Then, at the second step, the theoretical equation (4) was fitted to the experimental points of the PNC-effect as a function of the energy in the ranges (0.02 — 1.6) eV and (5,2 — 6.6) eV. In doing so, the same parameters of the s-resonances and the parameters of the p-resonances, obtained at the first step for these neutron energy ranges, were used. The only parameter in this fit was the nuclear matrix element of weak interaction, which was, in fact, the scale coefficient. The fitting parameters, obtained as a result of such a procedure, are presented in Table 2.

	$E_p$ (eV)	$\Gamma_p^{n1}$ (meV)	$\Gamma_p^r$ (meV)	$\Gamma_{p1/2}^{n1}/\Gamma_p^{n1}$	$\Delta\varphi_{sp}$	$(p H_w s) \cdot 10^4$ (eV)
1	0.20±0.03	0.48±0.15	178±55	1.00±0.01	0.97±0.30	3
2	0.38±0.02	0.05±0.03	60±50	0.50±0.20	1.55±0.30	9.5
3	1.20±0.02	0.17±0.08	163±20	0.63±0.10	-0.38±0.30	5
4	5.38±0.10	2.60±0.60	1040±15	0.99±0.01	-1.80±0.20	< 2
5	5.74±0.01	5.00±0.70	80±20	0.87±0.06	-1.57±0.15	< 6

Table 2: Main parameters of theoretical equations (3,4,5) obtained in combined fit of the PC (forward-backward and left-right) and PNC asymmetry effects as the functions of resonance neutron energies from the range (0.02–6.6) eV in  $^{235}\text{U}$  fission.

The parameters presented in Table 2 were found to be reasonably tolerant to additional s-resonances from outside the energy range investigated being involved in the analysis. As this takes place, the most stable data were obtained for the positions and widths of p-wave resonances. The phase factors usually include all of the inaccuracies of the main simplified assumptions and the fitting procedure as well. Unfortunately, because of the insufficient statistical accuracy of our data and the many fitting parameters, the independent stable information about  $K$ -values can not be extracted from an analysis of our data. The errors pointed out in Table 2 were obtained in the fitting procedure. The estimated errors for the matrix element values shown in the Table 2 were about 30%.

It can be seen from Fig 7 that a wholly satisfactory joint description of the PC and PNC interference effects has been achieved for  $^{235}\text{U}$  fission induced by low-energy resonance neutrons. The obvious scattering of some experimental points about the fitting curve far beyond statistical errors could not be eliminated by the introduction into the analysis of several additional p-resonances. The origin of this scattering of experimental points is not clear; it may be due to parameter  $K$ .

In conclusion we should point out the necessity of further investigations of the PNC effect in  $^{235}\text{U}$  fission for neutron energies higher than (1 — 2) eV. Such experiments could be carried out in Dubna at the new pulsed neutron source (Project IREN) [12] or in Los Alamos at LANSCE. It would also be interesting to perform similar PNC effect investigations for  $^{233}\text{U}$  and, especially, for  $^{239}\text{Pu}$  fission with the PC FB asymmetry interference effect as a function of neutron energy as was studied at IBR-30 reactor [20]. The density of excited levels in the  $^{240}\text{Pu}$  fissioning nucleus is well below that of  $^{236}\text{U}$  or  $^{234}\text{U}$ . As a result, the combined theoretical analysis of the interference effects in these nuclei would be more effective. Moreover, if one takes into account that these excited compound-states have the spins  $J = 0^+$  and  $1^+$ , it would be possible to examine the very interesting theoretical assumption about interference between them and the PNC effect which arises as a result of such interference in the vicinity of resonances with  $J = 0^+$  [4, 5].

## ACKNOWLEDGEMENTS

We are most grateful to all of our colleagues from the IBR-30 reactor department for keeping the reactor running in a stable condition during the course of the long physical measurements. We would also like to express our thanks to the management of the Neutron Research Department of PNPI RAS and the I.M. Frank Laboratory of Neutron Physics of JINR for the kind support of our work.

This work was made possible in part by Grant 93-02-3979 from the Russian Foundation for Basic Research, and Grants NOC000, NOC300, NK1000 and NK1300 from ISF and the Russian Government.

## REFERENCES

- [1] G.V. Danilyan, Usp. Fiz. Nauk **131** (1980) 329 [transl. Sov. Phys. Usp. **23** (1980) 323]
- [2] A.Ya. Alexandrovich, A.M. Gagarski, G.A. Petrov et al., Nucl. Phys. **A567** (1994) 541
- [3] A.M. Gagarski, G.A. Petrov, A. Koetzle et al., ILL experimental Report 3-07-74 (1996)
- [4] O.P. Sushkov and V.V. Flambaum, Usp. Fiz. Nauk **136** (1982) 3 [transl. Sov. Phys. Usp. **25** (1982) 1]
- [5] V.E. Bunakov and V.P. Gudkov, Nucl. Phys. **A401** (1983) 93
- [6] I.S. Shapiro, Usp. Fiz. Nauk **95** (1968) 647 [transl. Sov. Phys. Usp. **11** (1969) 4]
- [7] The Nucl. Fission Process, ed. C. Wagemans (CRC press, Boca Raton, 1991)
- [8] A.Ya. Alexandrovich, G.A. Petrov, G.V. Val'ski et al., J. de Phys. Colloq. **45** (1984) 83
- [9] G.A. Petrov, G.V. Val'ski, A.K. Petukhov et al., Nucl. Phys. **A502** (1989) 297
- [10] V.P. Alfimenkov, G.V. Val'ski, A.M. Gagarski et al., Yad. Fiz. **58** (1995) 799 [transl. Phys. Atom. Nucl. **58** (1995) 737]
- [11] S.F. Mughabghab et al., Neutron Cross Sections. NY. Acad. Press. V.1 (1981) Pt.A
- [12] V.L. Aksenov, N.A. Dikansky, V.L. Lamidze et al., Communications of JINR E3-92-110 Dubna (1992)
- [13] V.P. Alfimenkov, Yu.D. Mareev, L.B. Pikelner et al., J. Nucl. Phys., **54** (1991) 1489.
- [14] A.M. Gagarski, G.A. Petrov, A.K. Petukhov et al., Preprint LNPI 1634 Leningrad (1990)
- [15] V.P. Alfimenkov, A.M. Gagarski, G.A. Petrov et al., Preprint PNPI RAS NP-25-1996, 2117 Gatchina (1996)
- [16] G.V. Val'ski, I.S. Guseva, G.A. Petrov et al., Preprint PNPI RAS NP-83-1994 2025 Gatchina (1994)
- [17] V.V. Flambaum and G.F. Gribakin, Phys. Rev. **C50** (1994) 3122
- [18] A.M. Gagarski, S.P. Golosovskaya, G.A. Petrov et al., JETP Pis'ma **54** (1991) 9
- [19] A.M. Gagarski, S.P. Golosovskaya, A.B. Laptev et al., Preprint LNPI 1726 Gatchina (1991)
- [20] V.P. Alfimenkov, A.M. Gagarski, G.A. Petrov et al., Proc. ISINN-3 (1995) 276, Dubna
- [21] A.L. Barabanov and V.I. Furman, Proc. Intern. Conf. on Nucl. Data and Technology, Gatlinburg, Tennessee, v.1, p.448, 1994.
- [22] A.A. Bogdzel, W.I. Furman, N.N. Gonin et al., Preprint JINR, E3-96-220, Dubna, 1996

Received by Publishing Department  
on March 28, 1997.

Алфименков В.П. и др.

E3-97-106

Исследования нарушения четности и интерференционных эффектов при делении  $^{235}\text{U}$  резонансными нейтронами

Исследования эффекта нарушения четности в испускании осколков деления и интерференционных эффектов при измерении вперед-назад и лево-правой асимметрий были проведены на пучках нейтронов ИБР-30 в интервале энергий от 0,02 до 90 эВ. Впервые представлено согласованное теоретическое описание этих эффектов до уровня энергии 6,6 эВ. В результате были получены параметры  $p$ -волновых резонансов и впервые получены оценки матричных элементов слабого взаимодействия для делящихся ядер.

Работа выполнена в Лаборатории нейтронной физики им. И.М.Франка ОИЯИ.

Сообщение Объединенного института ядерных исследований. Дубна, 1997

Alfimenkov V.P. et al.

E3-97-106

Investigations of the Parity Violation and Interference Effects in  $^{235}\text{U}$  Fission Induced by Resonance Neutrons

Investigations of the PNC-effect of  $^{235}\text{U}$  fission fragment emission and interference effects of forward-backward left-right asymmetry were carried out on the neutron beams of the IBR-30 over the range of neutron energies from 0.02 to 90 eV. Satisfactory theoretical description of these effects below 6.6 eV was achieved for the first time. As a result of theoretical analysis, the main parameters of the  $p$ -wave resonances and the first estimates of the nuclear matrix elements of the weak interaction were extracted.

The investigation has been performed at the Frank Laboratory of Neutron Physics, JINR.

Communication of the Joint Institute for Nuclear Research. Dubna, 1997